Hindawi
Mathematical Problems in Engineering
Volume 2020, Article ID 2796590, 18 pages
https://doi.org/10.1155/2020/2796590

Research Article

Impedance with Finite-Time Control Scheme for Robot-Environment Interaction

Heyu Hu, Xiaoqi Wang, and Lerui Chen

School of Electronics and Information Engineering, Xi'an Jiaotong University, Xi'an 710049, China

Correspondence should be addressed to Heyu Hu; mylife00@126.com

Received 14 January 2020; Revised 7 April 2020; Accepted 30 April 2020; Published 25 May 2020

Academic Editor: Rafael Morales

For the robot system with the uncertain model and unknown environment parameters, a control scheme combining impedance and finite time is proposed. In order to obtain accurate force control performance indirectly by using position tracking, the control scheme is divided into two parts: an outer loop for force impedance control and an inner loop for position tracking control. In the outer loop, in order to eliminate the force tracking error quickly, the impedance control based on force is adopted; when the robot contacts with the environment, the satisfactory force tracking performance can be obtained. In the inner loop, the finite-time control method based on the homogeneous system is used. Through this method, the desired virtual trajectory generated by the outer loop can be tracked, and the contact force tracking performance can be obtained indirectly in the direction of force. This method does not need the dynamics model knowledge of the robot system, thus avoiding the online real-time calculation of the inverse dynamics of the robot. The unknown uncertainty and external interference of the system are obtained online by using the time-delay estimation, and the control process is effectively compensated, so the algorithm is simple, the convergence speed is fast, and the practical application is easy. The theory of finite-time stability is used to prove that the closed-loop system is finite-time stable, and the effectiveness of the algorithm is proved by simulations.

1. Introduction

Industrial robots are widely implemented in various fields and can perform complex tasks. In the production process that requires contact with the environment, the position control can no longer meet the requirements, such as polishing and deburring. It is not only necessary to control the end position of the robot but also to control the force generated when the robot contacts with the environment [1, 2]. In order to achieve compliant control, Hogan proposed impedance control [3]. By adjusting the mass, damping, and stiffness parameters at the end of the robot, it holds the force and position within a frame and maintains an ideal mechanical impedance relationship. Compared with hybrid force/position control [4], impedance control is an indirect method with strong robustness for some uncertainties and interference factors.

The accuracy of impedance control depends on the accurate understanding of the robot model and environment knowledge. However, in the actual robot-environment system, due to the existence of uncertainties and interference terms, it is difficult to get an accurate dynamic model and environmental parameters, which leads to great position and force errors in impedance control. It cannot be applied in many occasions with high control accuracy requirements, which is a major defect of impedance control relative to hybrid force/position control [5]. Seraji et al. proposed direct and indirect adaptive tracking impedance control methods, both of which have better force tracking effect when the environmental parameters are unknown, but they are not conducive to practical application due to adjusting too many adaptive gain parameters [6]. For the position tracking error caused by the imprecise dynamic model of the robot, Seul thinks that the expected force should be added to track the contact force directly, and the controller should have enough robustness to deal with the uncertainty of stiffness and position in the unknown environment, so an adaptive impedance control algorithm is proposed [7–9]. In order to

reduce the force tracking error caused by the uncertainty of the environmental position, Duan et al. [10] proposed an adaptive variable impedance control method based on the online adjustment of the impedance parameters of the tracking error, in order to compensate the unknown environment and the dynamic expected force, and achieved a better control effect. Inspired by the fact that human beings can adjust the limb impedance to interact with various environments stably, Dong et al. established an estimation model for the uncertainty and interference term of the robot, thus improving the interaction ability between the robot and the environment [11]. Li et al. used the method of iterative learning to obtain the parameters of impedance control and realized the contact control between the robot and an unknown environment [12]. Although the above method can achieve high-precision force tracking and position tracking, the calculation of debugging parameters should be strict; otherwise, the system stability will be seriously affected. In addition, recent studies have shown that it is difficult to improve the robustness of modeling errors without losing the accuracy of the desired impedance. This is known as the "accuracy/robustness paradox" in impedance control [13].

In order to ensure the stability and robustness and realize the precise control of the robot's position and force at the same time, adaptive sliding mode control is proposed in [14], which has good tracking performance in the case of small chattering. In [15], the traditional nonsingular terminal sliding mode control strategy is developed, and a continuous terminal sliding mode controller is designed to realize the continuous finite-time stable tracking control of a nonlinear robot system. In [16], the continuous sliding mode tracking problem of the robot under parameter uncertainty and external disturbance is studied. A chatter-free integral terminal sliding mode control scheme is proposed, which combines the integral terminal sliding mode surface with the observer.[17]. This strategy is very attractive to the robot system designed for position adjustment and has been widely used. In this strategy, impedance control is used to determine the virtual desired trajectory. Then, the position control loop is used to track the virtual desired trajectory, and the control target becomes trajectory tracking, which has been widely studied in the past decades.

Due to the uncertainty and disturbance of the robot model [18], many classical nonlinear control methods are applied to the position control of the inner loop, such as sliding mode, backstepping, and adaptive. Different from the asymptotic convergence of traditional control methods, finite-time control means that the system state can converge to the equilibrium point in finite time [19, 20], so it has faster instantaneous response characteristics and higher tracking accuracy and has better robustness and anti-interference performance, especially suitable for the high-quality control of the nonlinear industrial robot system [21]. At present, it has been widely used in the field of industrial control [22, 23]. The common finite-time control methods include the homogeneous system method, finite-time Lyapunov function construction method, and terminal sliding mode control [24–26]. The sliding mode control method of the nonsingular terminal based on time-delay estimation proposed in [27] does not need the knowledge of the dynamic model of the robot, and the algorithm is simple and effective but uses saturation function to eliminate "chattering" and sacrifices the control accuracy. In [28], a finite-time stable robot control method proposed by combining PD and gravity compensation strategy is globally stable in the sense of state feedback but locally finite-time stable in the sense of output feedback. In [29], a kind of nonlinear PD controller proposed for the robot is globally finite-time stable. It only replaces the linear position error term of traditional PD control with the fractional power form of error but obtains better control performance. In [30], a global finite-time tracking control scheme based on the inverse dynamics method is proposed, which is also a modification of the traditional inverse dynamics method of the robot. The global finite-time stability is proved by the principle of LaSalle invariant set and the theory of finite-time stability, and the simulation results show that the method has faster response speed. In [31], based on the terminal sliding mode control, using the advantages of fast terminal sliding mode control and the neural network, a finite-time tracking control scheme of the robot is proposed. At present, the control methods combined with finite time are adaptive [32], sliding mode [33], observer [34], and so on. Time-delay estimation [35] is applied to estimate unknown robot dynamics and external interference. In order to ensure the correctness of the time-delay function, the time delay L must be small enough, usually set as the sampling time. Current hardware and computer technology fully meet the requirements, but the time-delay estimation method has been rarely used in the nonlinear robot control system since it was proposed. In the current literature, there is no finite-time control method for the position control of the robot's inner loop. On the basis of [30], using the method of time-delay estimation, we design a continuous finite-time stable control strategy, which can also obtain high-precision trajectory tracking control without knowing the dynamics model of the robot.

In order to solve the problem of position/force control when the robot is interacted with an uncertain model and unknown environmental parameters, a dual-loop control strategy based on impedance control and finite-time control is proposed in this paper. The outer loop is force-based impedance control, which is used for force compliance control and virtual ideal trajectory generation; the inner loop is the position control based on finite time, which solves the problem of model uncertainty and unknown environmental parameters and makes the end trajectory of the robot track the virtual ideal trajectory generated by the outer loop. This method does not depend on the model of the robot and environment. By setting impedance parameters and finite-time control parameters, it can achieve an ideal control effect. Based on the Lyapunov stability theorem, the stability of the closed-loop system is proved. Therefore, we believe that this paper has the main contributions in the following:

(1) In order to facilitate the position/force tracking impedance control of the robot system, a double closed-loop control structure is proposed, that is, the

outer loop for force impedance control and the inner loop for position tracking control

(2) In the outer loop, we implement impedance control to make the contact force between the end of the robot and the environment show compliance and generate the virtual desired trajectories

(3) In the inner loop, finite-time control is applied to solve the unknown parameters and dynamic uncertainties

This paper includes the following contents. In Section 2, the system model is introduced, including the kinematics model and dynamic model. In Section 3, the details of the proposed algorithm are presented. In Section 4, simulations with different control objectives are conducted to verify the feasibility of the proposed method. In Section 5, concluding remarks are given.

2. Theoretical Foundations

2.1. Finite-Time Stability. Since the finite-time control system is a non-Lipshitz continuous system, common theories to determine the stability of the system, such as Lyapunov inverse theorem or invariant set principle, cannot be applied directly. The finite-time homogeneous theory and the finite-time Lyapunov stability theory and related concepts to determine the finite-time stability theorem are introduced as follows.

Consider the following systems:

$$\dot{x} = f(x),\ f(0) = 0, \tag{1}$$

where $x \in R^n$ and $f: U \longrightarrow R^n$ is a continuous function defined in the domain U to the n-dimensional space R^n.

Definition 1. Let $f(x)$: $R^n \longrightarrow R^n$ be a vector function; for any $\varepsilon > 0$, there exists $(r_1, r_2, \ldots, r_n) \in R^n$, where $r_i > 0 \quad (i = 1, 2, \ldots, n)$, so that $f(x)$ satisfies

$$f_\varepsilon(\varepsilon^{r_1}x_1, \ldots, \varepsilon^{r_n}x_n) = \varepsilon^{k+r_i} f_i(x), \quad i = 1, 2, \ldots, n, \tag{2}$$

where $k \geq -\max\{r_i, i = 1, 2, \ldots, n\}$ and $f(x)$ is considered to have homogeneous degree k with respect to $(r_i, r_2, \ldots, r_n)$.

Definition 2. Let $V(x)$: $R^n \longrightarrow R$ be a continuous scalar function; for any $\sigma > 0$, there is $(r_1, r_2, \cdots, r_n) \in R^n$, where $r_i > 0 \quad (i = 1, 2, \ldots, n)$, so that $f(x)$ satisfies

$$V_i(\varepsilon^{r_1}(x), \ldots, \varepsilon^{r_n}x_n) = \varepsilon^\sigma V(x), \quad \forall x \in R^n. \tag{3}$$

Then, $V(x)$ is said to have homogeneous degree σ with respect to $(r_i, r_2, \ldots, r_n)$.

The criterion theorems of finite-time stability are as follows:

Theorem 1. *If the system represented by equation (1) has homogeneous degree $k < 0$ and is globally asymptotically stable, then the system is globally finite-time stable, and $x = 0$ is the equilibrium point of the system.*

Theorem 2. *The closed-loop system with global asymptotic stability and local finite-time stability is globally finite-time stable.*

2.2. Kinematics and Dynamics Model. The kinematics equation of the robot is

$$X = P(q). \tag{4}$$

Among them, $X \in R^m$ represents the position in the task space, $q \in R^n$ represents the position of the joint angle, and $P(\cdot)$ is a mapping matrix of forward kinematics, which usually represents the transformation relationship between task space and joint space. Equation (4) is differentiated to obtain the velocity vector at the end of the robot:

$$\dot{X} = J\dot{q}, \tag{5}$$

where $J \in R^{m\times n}$ represents the Jacobian matrix. Equation (5) is differentiated to obtain the acceleration vector at the end of the robot:

$$\ddot{X} = J\ddot{q} + \dot{J}\dot{q}. \tag{6}$$

From equations (4)–(6), the relationship between joint space velocity and acceleration can be obtained:

$$\dot{q} = J^*\dot{X} + (I - J^*J)v, \tag{7}$$

$$\ddot{q} = J^*(\ddot{X} - \dot{J}\dot{q}) + (I - J^*J)v, \tag{8}$$

where $J^* = J^{\mathrm{T}}(JJ^{\mathrm{T}})^{-1}$ represents the pseudo-inverse of the Jacobian matrix J and v is any vector. In this paper, we take the minimum norm solution, at this time, $v = 0$.

For a multi-input and multioutput n-DOF joint robot, its dynamic equation can be expressed as follows:

$$M(q)\ddot{q} + C(q, \dot{q})\dot{q} + G(q) + J^{\mathrm{T}}F_e = \tau, \tag{9}$$

where, $q, \dot{q}, \ddot{q} \in R^n$ are the joint angle, angular velocity, and angular acceleration vectors, respectively, $\tau \in R^n$ is the control torque of each joint, $F_e \in R^n$ is the contact force vector between the end of the robot and the environment, $M(q) \in R^{n\times n}$ is the symmetric positive-definite inertia matrix, $C(q, \dot{q}) \in R^n$ is the Coriolis force and centripetal force matrix, and $G(q) \in R^n$ is the gravity vector.

From equations (5)–(9), we can get

$$\overline{M}\ddot{q} + H(q, \dot{q}, \ddot{q}) + J^{\mathrm{T}}F_e = \tau, \tag{10}$$

$$H(q, \dot{q}, \ddot{q}) = (M(q) - \overline{M})\ddot{q} + C(q, \dot{q})\dot{q} + G(q), \tag{11}$$

where $\overline{M}$ is the estimated value of $M(q)$. $H(q, \dot{q}, \ddot{q})$ is an uncertain term and expression.

2.3. Problem Statement. In this paper, a control strategy combining the inner loop and outer loop is developed for controlling the robot-environment interaction, as shown in Figure 1. Particularly, the target impedance model is defined as

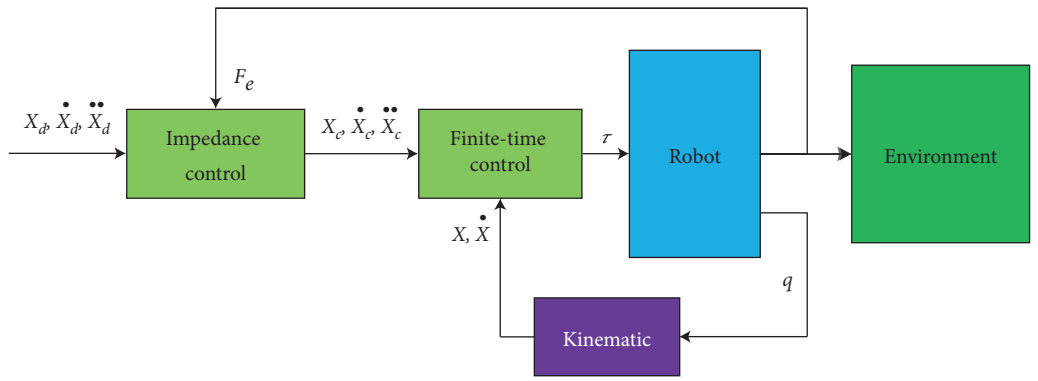

Figure 1: Control block diagram.

$$M_d\left(\ddot{X}_d - \ddot{X}_c\right) + B_d\left(\dot{X}_d - \dot{X}_c\right) + K_d\left(X_d - X_c\right) = F_e, \tag{12}$$

where M_d, B_d, and K_d represent the desired inertia, damping, and stiffness matrices, X_d represents the desired trajectory, and X_c represents the virtual desired trajectory for the loop of position control. We should find the impedance parameters to achieve the desired interaction performance and consider the environment dynamics. However, in many situations, accurate models of the environment are almost impossible to obtain. In this regard, we aim to apply the finite-time law for position control, which can make the system track the virtual desired trajectory. As position control is applied to make $X \longrightarrow X_c$ as $t \longrightarrow \infty$, the impedance model becomes

$$M_d\left(\ddot{X}_d - \ddot{X}\right) + B_d\left(\dot{X}_d - \dot{X}\right) + K_d\left(X_d - X\right) = F_e. \tag{13}$$

Note that, according to equation (12), only the virtual desired trajectory X_c is refined, and the external loop of impedance control cannot affect the control performance of the inner loop. In the following sections, the proposed impedance control and position control are described in detail.

3. Control Scheme

We take the following control strategy. F_e is measured by a six-axis force/moment sensor installed at the end of the robot, and q is measured by an angle encoder installed on the robot body.

3.1. Impedance Control. In the outer loop of impedance control, the control objective is to generate an ideal given trajectory with a balanced trajectory. The following impedance equation can be established [30]:

$$M_d\ddot{X}_c + B_d\dot{X}_c + K_dX_c = -F_e + M_d\ddot{X}_d + B_d\dot{X}_d + K_dX_d, \tag{14}$$

where $X_c(0) = X_d(0)$ and $\dot{X}_c(0) = \dot{X}_d(0)$.

Among them, $M_d(t)$, $B_d(t)$, and $K_d(t)$ are positive definite matrices, which are the inertia matrix, damping matrix, and stiffness matrix of the expected impedance model, respectively. The diagonal elements of these expected impedance model matrices describe the mechanical characteristics required in the contact process of the robot and can be selected accordingly to the given operation tasks.

3.2. Design of the Finite-Time Controller. The purpose of finite-time trajectory tracking control of the robot is to make the trajectory X of the robot effectively track the expected virtual control trajectory X_c and make the tracking error e converge to 0 in finite time, where $e(t)$ and $\dot{e}(t)$ are defined as follows:

$$\begin{aligned} e &= X - X_c, \\ \dot{e} &= \dot{X} - \dot{X}_c. \end{aligned} \tag{15}$$

In order to facilitate the design and analysis of the controller, we define the vector of $\mathrm{Sat}_\gamma(\xi) = (\mathrm{sat}(\xi_1), \ldots, \mathrm{sat}(\xi_n)^{\mathrm{T}})$, where $\mathrm{sat}(\xi_i)$ is the saturation function:

$$\mathrm{Sat}(x) = \begin{cases} 1, & x > 1, \\ x, & |x| \le 1, \\ -1, & x < -1. \end{cases} \tag{16}$$

The vector $\mathrm{Sig}(\cdot)^\alpha$ is defined as follows:

$$\mathrm{Sig}(X)^\alpha = \mathrm{Sig}(X)^\alpha = \left[\left|X_1\right|^\alpha \mathrm{sgn}(X_1), \ldots, \left|X_n\right|^\alpha \mathrm{sgn}(X_n)\right]^{\mathrm{T}}. \tag{17}$$

where $X = [X_1, \ldots X_n]^{\mathrm{T}}$, $0 < \alpha < 1$, and $\mathrm{sgn}(\cdot)$ is a standard symbolic function defined as follows:

$$\mathrm{sgn}(x) = \begin{cases} 1, & x > 0, \\ 0, & x = 0, \\ -1, & x < 0. \end{cases} \tag{18}$$

The control law of the robot is designed as follows:

$$\tau = \overline{M}J^*\left(u - \dot{J}\dot{q}\right) + \hat{H}\left(q, \dot{q}, \ddot{q}\right) + J^{\mathrm{T}}F_e, \tag{19}$$

where

$$u = X_c - K_p \mathrm{Sat}\left(\mathrm{Sig}(e)^{\alpha_1}\right) - K_b \mathrm{Sat}\left(\mathrm{Sig}(\dot{e})^{\alpha_2}\right), \tag{20}$$

where K_p and K_b are normal number diagonal matrices, $0 < \alpha_1 < 1$, and $\alpha_2 = 2\alpha_1/(\alpha_1 + 1)$. $\widehat{H}(q, \dot{q}, \ddot{q})$ is the estimated value of $H(q, \dot{q}, \ddot{q})$, which is obtained online through time-delay estimation, as shown in the following equation:

$$\widehat{H}(q, \dot{q}, \ddot{q}) = H_{t-L}(q, \dot{q}, \ddot{q}), \tag{21}$$

where $H_{t-L}(q, \dot{q}, \ddot{q})$ is defined as the time-delay estimate of $H(q, \dot{q}, \ddot{q})$ and L is the estimated delay time. In practical application, the minimum L that can be set is the sampling period. According to equation (11),

$$H_{t-L}(q, \dot{q}, \ddot{q}) = \tau_{t-L} - \left(J^{\mathrm{T}} F_e\right)_{t-L} - \overline{M}\ddot{q}_{t-L}. \tag{22}$$

Combined with the above equations (19)–(22), the control law can be expressed as follows:

$$\begin{aligned}\tau = \tau_{t-L} - \overline{M}\ddot{q}_{t-L} + \overline{M}J^*\Big(&\ddot{X}_c - K_p \mathrm{Sat}\left(\mathrm{Sig}(e)^{\alpha_1}\right) \\ &- K_b \mathrm{Sat}\left(\mathrm{Sig}(\dot{e})^{\alpha_2}\right) - \dot{J}\dot{q}\Big) + J^{\mathrm{T}} F_e.\end{aligned} \tag{23}$$

It can be seen that the control law does not need the knowledge of the dynamics model of the robot, so the algorithm is simple. According to equation (23), $H(q, \dot{q}, \ddot{q})$ with actual dynamic terms can be estimated in real time by using the past control input and joint acceleration. Generally, joint acceleration at $t - L$ time can be calculated by the following equation:

$$\ddot{q}_{t-L} = \frac{q_{t-L} - 2q_{t-2L} + q_{t-3L}}{L^2}. \tag{24}$$

Obviously, equation (24) is also quite simple, so it is particularly suitable for robot control.

3.2.1. Global Finite-Time Stability Analysis. For the above finite-time control law, we have the following global continuous finite-time stability theorem.

Theorem 3. *For given industrial robot system (9), a control law (23) based on time-delay estimation is adopted to realize the global finite-time stability of the position and speed tracking errors of the closed-loop system, namely,*

$$\begin{aligned}\lim_{t \longrightarrow T(X_0)} e(t) = 0, \\ \lim_{t \longrightarrow T(X_0)} \dot{e}(t) = 0,\end{aligned} \tag{25}$$

where $T(X_0)$ is the convergence time function of the initial state X_0 of the system, and $X_0 = X(0) = \left[e(0)^T \;\; e(0)^T\right]^T \in R^{2n}$.

The proof of the theorem is divided into two steps. First, it is proved to be globally asymptotically stable according to the LaSalle invariant set principle; second, it is proved to be globally finite-time stable according to Theorem 1 or Theorem 2.

(1) Global Asymptotic Stability. By substituting the control input (23) into dynamic equation (9) of the robot and combining equation (20), we can get

$$\begin{aligned}\ddot{e} = &-K_p \mathrm{Sat}\left(\mathrm{Sig}(e)^{\alpha_1}\right) - K_b \mathrm{Sat}\left(\mathrm{Sig}(\dot{e})^{\alpha_2}\right) \\ &- \overline{M}^{-1}\left[H(q, \dot{q}, \ddot{q}) - H_{t-L}(q, \dot{q}, \ddot{q})\right].\end{aligned} \tag{26}$$

Here, δ is defined as the time-delay estimation error, namely,

$$\delta = \overline{M}^{-1}\left[H(q, \dot{q}, \ddot{q}) - H_{t-L}(q, \dot{q}, \ddot{q})\right]. \tag{27}$$

When the robot works in the unsaturated region, equation (26) can be written as

$$\ddot{e} = -K_p \mathrm{Sig}(e)^{\alpha_1} - K_b \mathrm{Sig}(\dot{e})^{\alpha_2} - \delta. \tag{28}$$

When the robot works in the saturated region, equation (26) can be written as $\ddot{e} = -\delta$. Obviously, we can only discuss equation (28) to meet the requirements.

The following nonnegative Lyapunov functions are used:

$$V = \frac{1}{2}\dot{e}^{\mathrm{T}}\dot{e} + \frac{1}{\alpha_1 + 1}\sum_{i=1}^{n} k_{pi}\left|e_i\right|^{\alpha_1 + 1}, \tag{29}$$

where k_{pi} is the ith diagonal element of the diagonal matrix K_p and e_i is the ith component of the tracking error e.

For V, the derivative of time t is obtained:

$$\dot{V} = \dot{e}^{\mathrm{T}}\ddot{e} + \dot{e}^{\mathrm{T}} K_p \mathrm{Sig}(e)^{\alpha_1}. \tag{30}$$

If equation (28) is brought in, the following can be obtained:

$$\begin{aligned}\dot{V} &= \dot{e}^T\left(\ddot{e} + K_p \mathrm{Sig}(e)^{\alpha_1}\right) \\ &= \dot{e}^T\left(-K_p \mathrm{Sig}(e)^{\alpha_1} - K_b \mathrm{Sig}(\dot{e})^{\alpha_2} - \delta + K_p \mathrm{Sig}(e)^{\alpha_1}\right) \\ &= -\dot{e}^T\left(K_b \mathrm{Sig}(\dot{e})^{\alpha_2}\right) + \delta \\ &= -\dot{e}^T\left[K_b|\dot{e}|^{\alpha_2}\mathrm{sgn}(\dot{e}) + \delta\right].\end{aligned} \tag{31}$$

It can be seen that if

$$\left|\delta_i\right| \le k_{bi}\left|\dot{e}_i\right|^{\alpha_2}, \tag{32}$$

where k_{bi} is the ith diagonal element of the diagonal matrix K_d, then $\dot{V} \le 0$. According to the principle of the LaSalle invariant set, the system is asymptotically stable. Jin et al. [27] show that the time-delay estimation error δ is bounded.

According to equation (28), δ is a bounded nonlinear term related to e; equation (32) means that when $e = 0$, $\delta = 0$ must be met. Therefore, if the appropriate constant matrix $\overline{M}$ and delay time L can be selected for equation (32), the stability of the system can be guaranteed.

(2) Finite-Time Stability. In order to prove that the time-delay error δ is a bounded system interference, we first assume that $\delta = 0$, and let $x_1 = e$, $x_2 = \dot{x}_1 = \dot{e}$, and $x = (x_1^{\mathrm{T}}, x_2^{\mathrm{T}})^{\mathrm{T}}$. Then, equation (31) can be rewritten as

$$\begin{cases}\dot{x}_1 = x_2, \\ \dot{x}_2 = -K_p \mathrm{Sig}\left(x_1\right)^{\alpha_1} - K_b \mathrm{Sig}\left(x_2\right)^{\alpha_2}.\end{cases} \tag{33}$$

Obviously, $x = 0$ is the equilibrium point of equation (28). According to Definition 1, it is easy to prove that the homogeneous degree of system (28) with respect to $r_1 = 2$

Table 1: Model parameters of the robot.

Identifier	Length (m)	Distance (m)	Angle (°)	Mass (kg)	Inertia matrix (kg · m^2)
1	0	0	0	0.1	[0, 0.35, 0, 0, 0, 0]
2	0	1.08	−90	17.4	[0.13, 0.524, 0.539, 0, 0, 0]
3	0.1505	0.0203	90	4.8	[0.066, 0.086, 0.0125, 0, 0, 0]
4	0.645	0	−90	0.82	[1.8e − 3, 1.3e − 3, 1.8e − 3, 0, 0, 0]
5	0	0	0	0.34	[0.3e − 3, 0.4e − 3, 0.3e − 3, 0, 0, 0]
6	0	0	0	0.09	[0.15e − 3, 0.15e − 3, 0.04e − 3, 0, 0, 0]

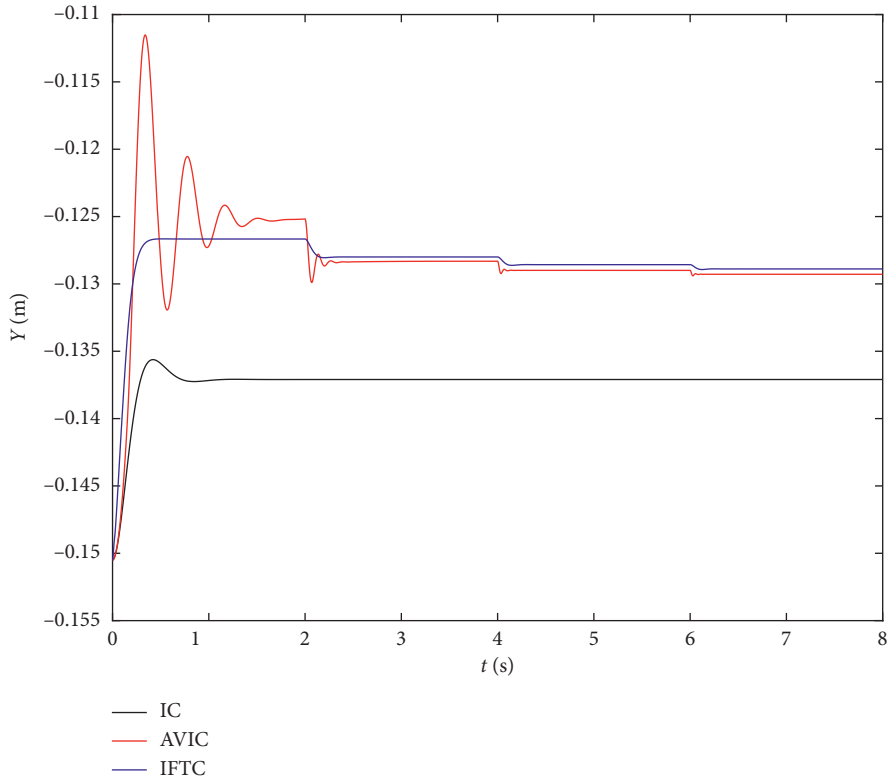

Figure 2: Position tracking on planes.

and $r_2 = \alpha_1 + 1$ is $k = \alpha_1 - 1 < 0$. From Theorem 1, it can be seen that closed-loop system (17) is globally finite-time stable. However, due to the existence of the time-delay estimation error δ, the steady-state error of the system eventually converges to the region Ω within the finite time, and the convergence region Ω of the steady-state error of the system is in nonlinear proportion to the control gain K_b of the system and in nonlinear proportion to the upper bound d of δ [36]. Therefore, as long as K_d is adjusted to ensure that $k_{\text{bi}} > k_{\text{bi}}$, the required tracking accuracy and antidisturbance index can be met. Since the sampling period of most servo systems can reach 0.2 ms, $H_{t-L}(q, \dot{q}, \ddot{q})$ is very close to $h(q, \dot{q}, \ddot{q})$, and the ideal state close to $\delta = 0$ can be obtained in practical application, so the above assumption $\delta = 0$ is in line with the reality.

In conclusion, for given nonlinear robot system (9), the finite-time control law (13) based on time-delay estimation proposed by the author is adopted. The system converges to the neighbourhood Ω of $e(t) = 0$ and $\dot{e}(t) = 0$ in finite time.

4. Simulation Study

In this chapter, simulations are designed to verify the proposed control algorithm and its performance. The simulations include a series of typical application scenarios, covering most of the actual situations. The simulations are conducted in the Matlab/Simulink environment. The robot model and the contact model are obtained in Section 2, and the parameters are shown in Table 1. For simplicity, the simulation assumes that the contact exists only in the Y direction. The control block diagram is shown in Figure 1.

The contact between the robot and the environment includes two stages: contact space and free space. In the contact space, the magnitude of the contact force is related to the relative displacement, relative velocity, stiffness, and damping of the contact surface. In the free space, the contact force is 0. Definition error is

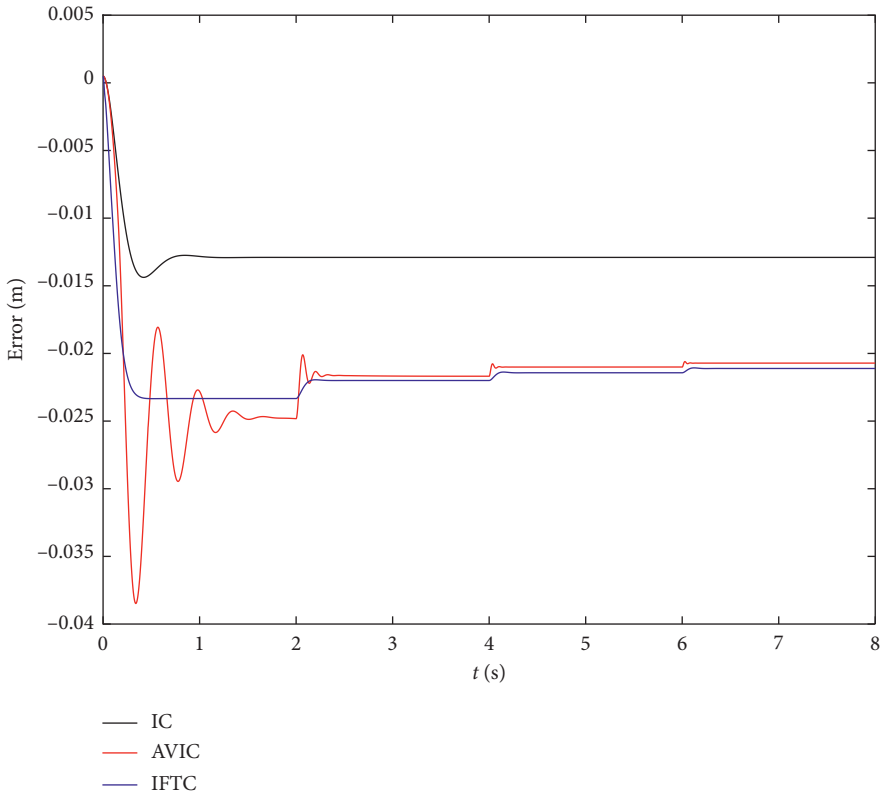

Figure 3: The trajectory tracking error on planes.

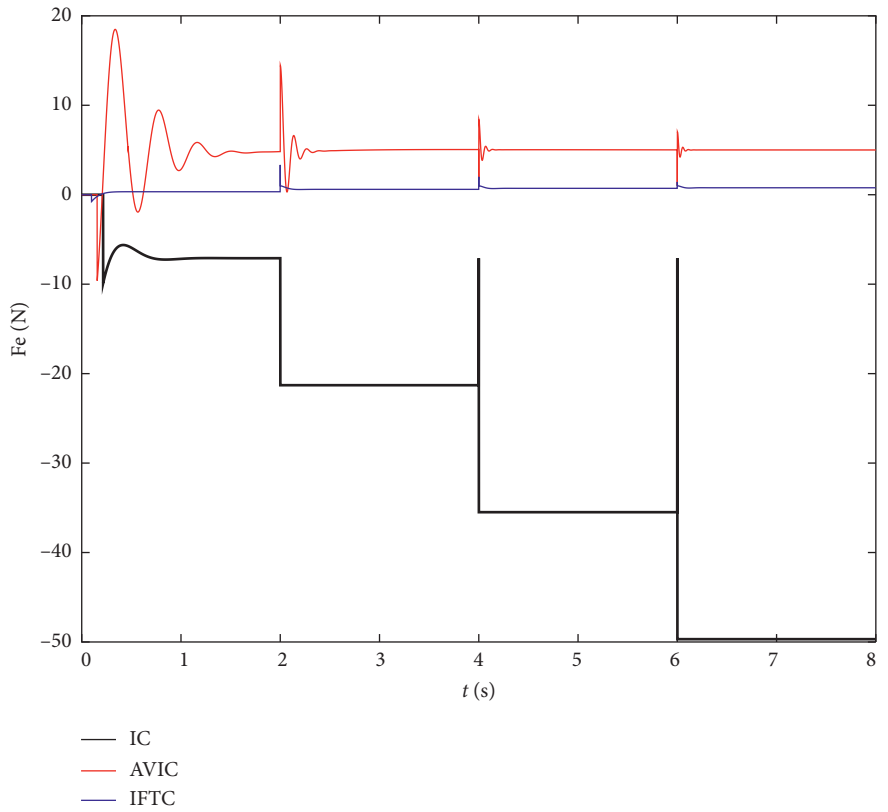

Figure 4: Force tracking on planes.

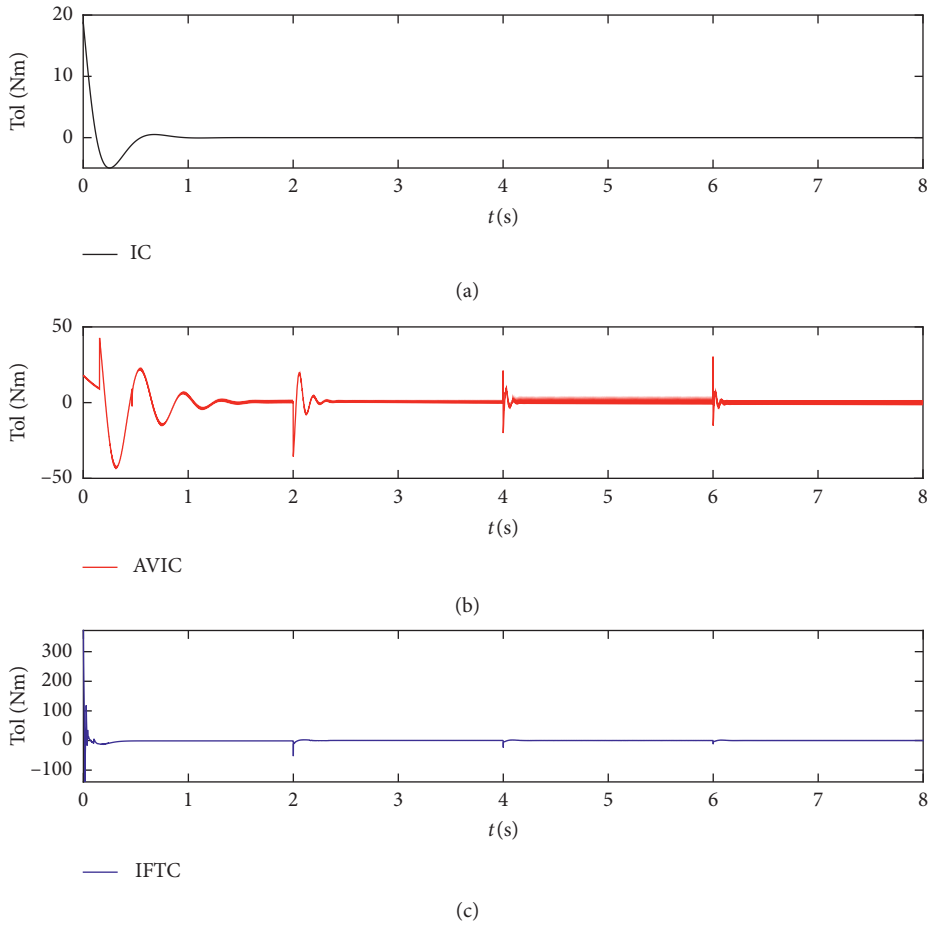

Figure 5: The torque of the first joint on planes.

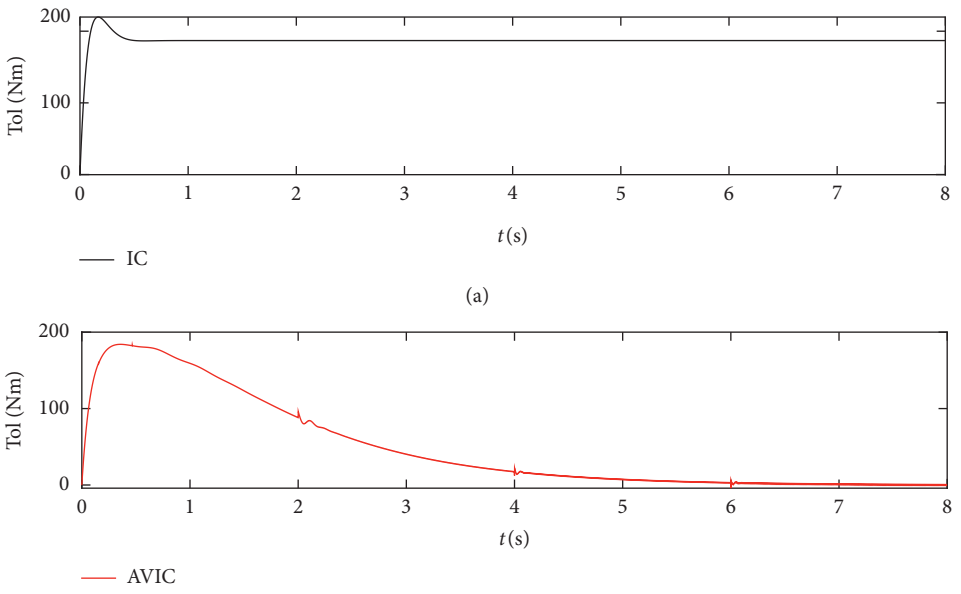

Figure 6: Continued.

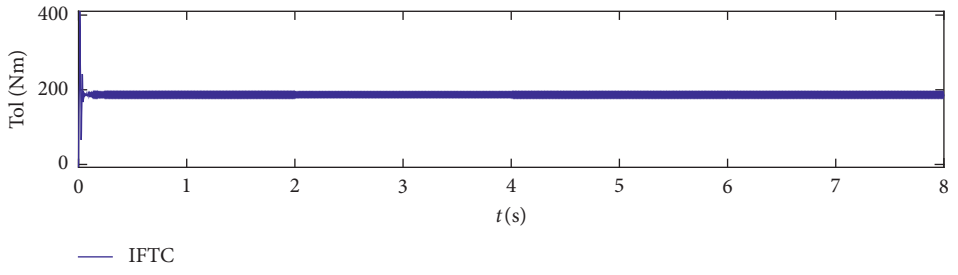

(c)

Figure 6: The torque of the second joint on planes.

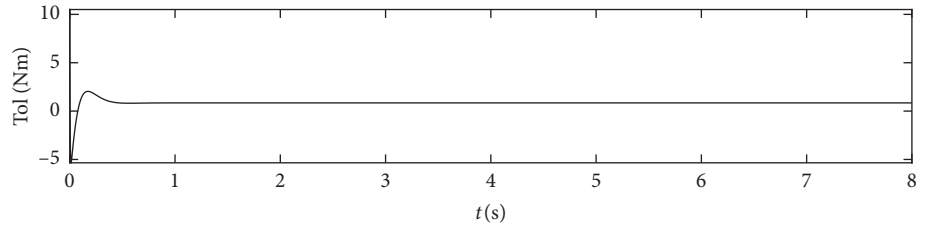

(a)

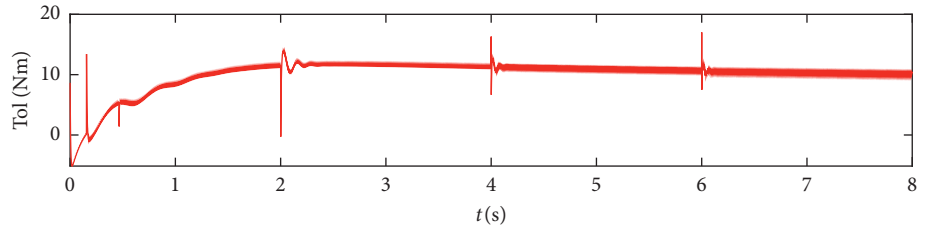

(b)

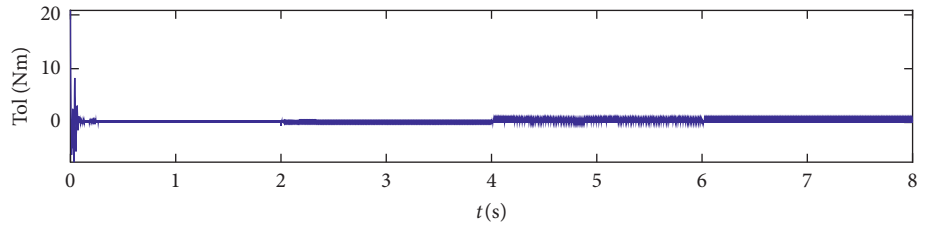

(c)

Figure 7: The torque of the third joint on planes.

$$\begin{aligned} \nabla x &= x - x_e, \\ F_e &= B_e \cdot F_1(\Delta x, \Delta \dot{x}) + K_e \cdot F_2(\Delta x), \end{aligned} \tag{34}$$

where x_e represents the contact position, B_e and K_e represent the damping and stiffness of the contact surface, respectively, F_e represents the contact force, and Δx represents the relative distance. If Δx is positive or negative when penetrating the contact surface, $\Delta \dot{x}$ is its derivative. When $\Delta x > 0$, $F_1(\Delta x, \Delta \dot{x}) = \Delta \dot{x}$, $F_2(\Delta x) = \Delta x$, and $\Delta x \le 0$, $F_1(\Delta x, \Delta \dot{x}) = 0$ and $F_2(\Delta x) = 0$.

The main content includes impedance with finite-time control (IFTC, the proposed method in this paper), adaptive variable impedance control (AVIC, proposed by Seul et. al. [7]), and the typical impedance control (IC). The interference is not considered.

The basic parameters are as follows: the initial position is $(1.10, -0.150, 0.645)$, and the initial attitude angle is $(0, 0, 0)$. Impedance coefficients are $M_d = (1, 1, 1, 1, 1, 1)$, $B_d = (30, 30, 30, 30, 30, 30)$, and $K_d = (10, 10, 10, 10, 10, 10)$. Finite-time parameters are $K_b = (20, 20, 20, 20, 20, 20)$ and $K_p = (500, 500, 500, 500, 500, 500)$.

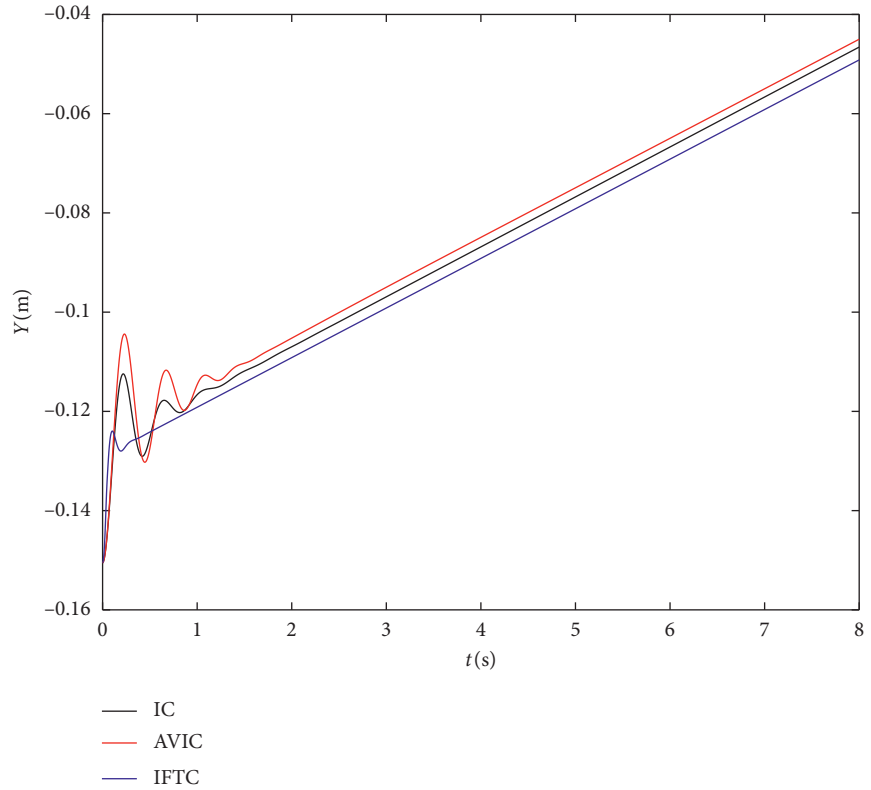

Figure 8: Position tracking on the slope surface.

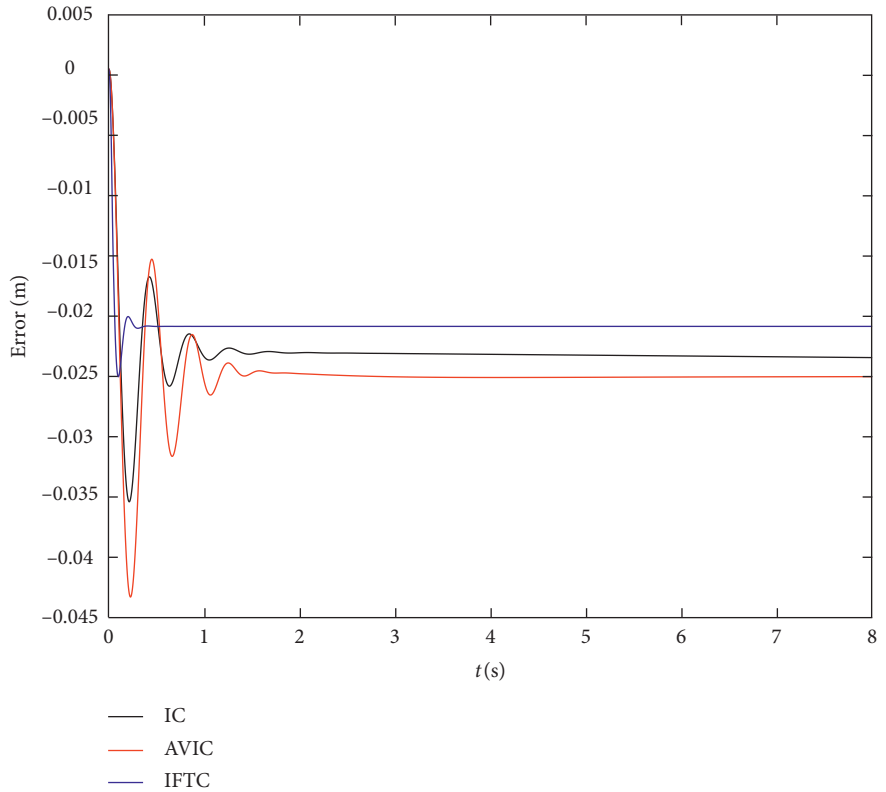

Figure 9: The trajectory tracking error on the slope surface.

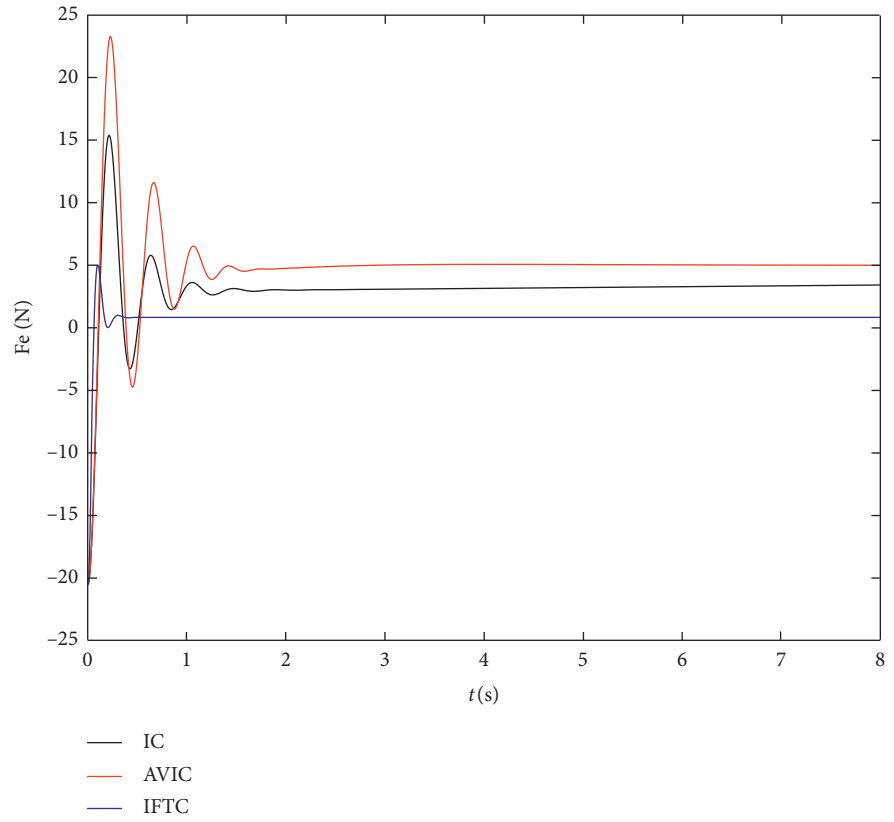

Figure 10: Force tracking on the slope surface.

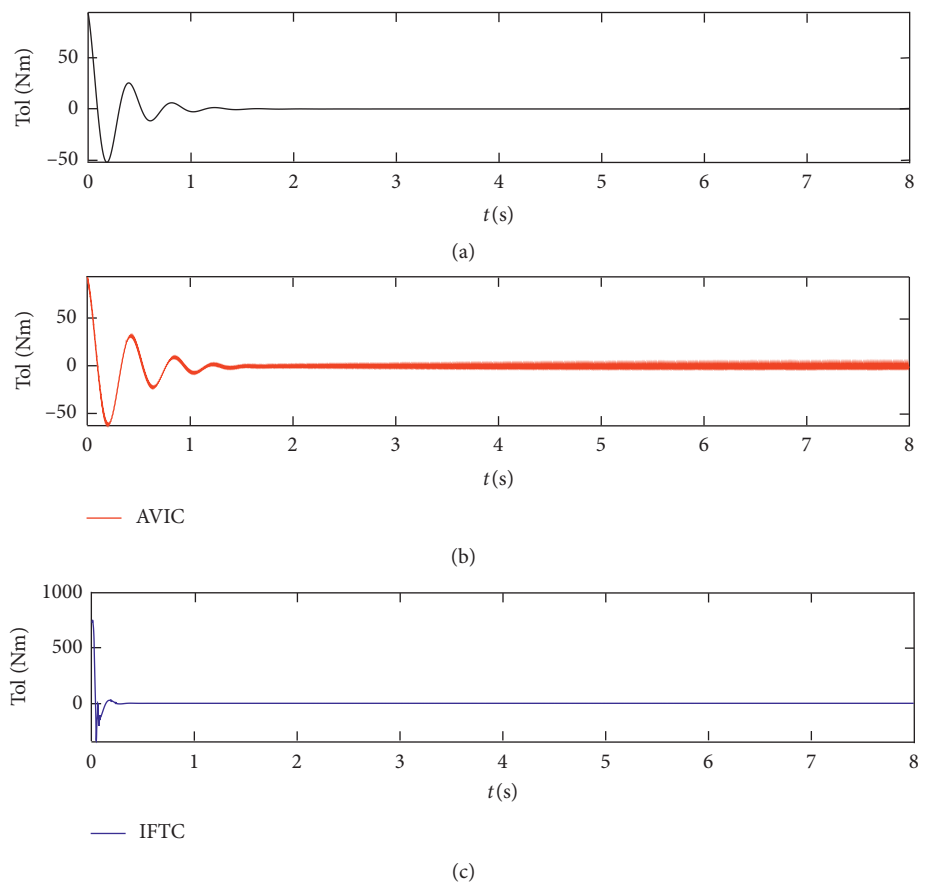

Figure 11: The torque of the first joint on the slope surface.

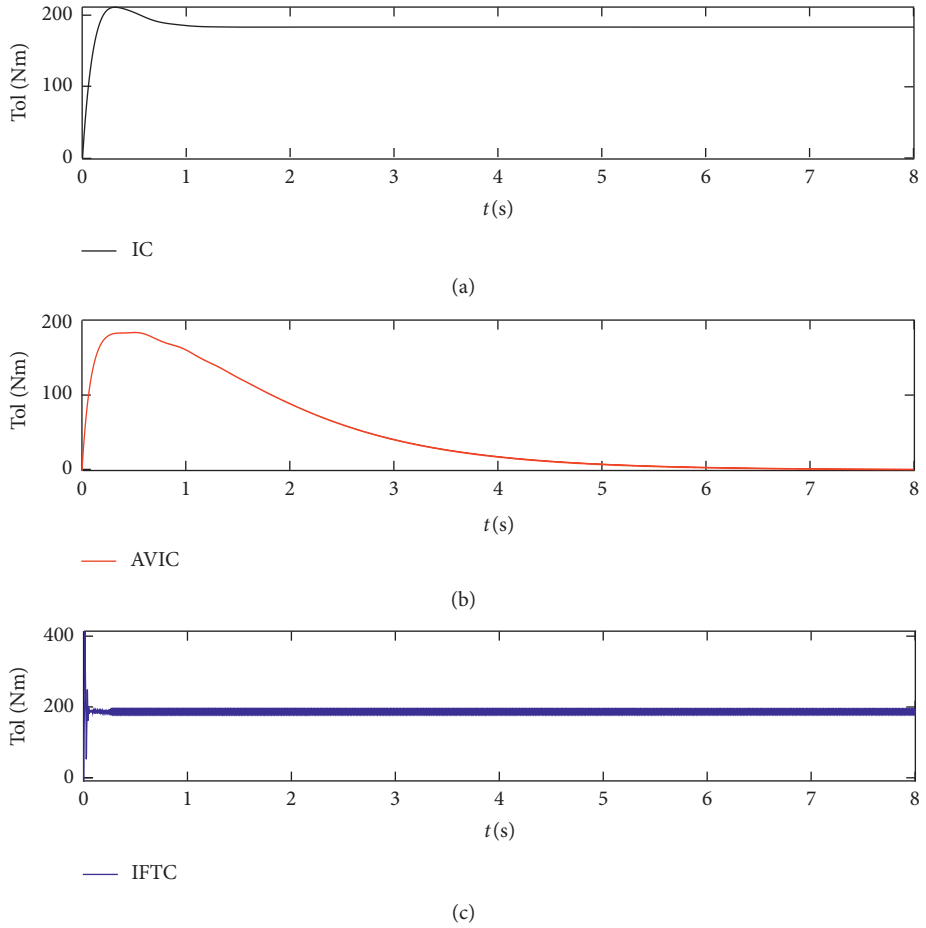

Figure 12: The torque of the second joint on the slope surface.

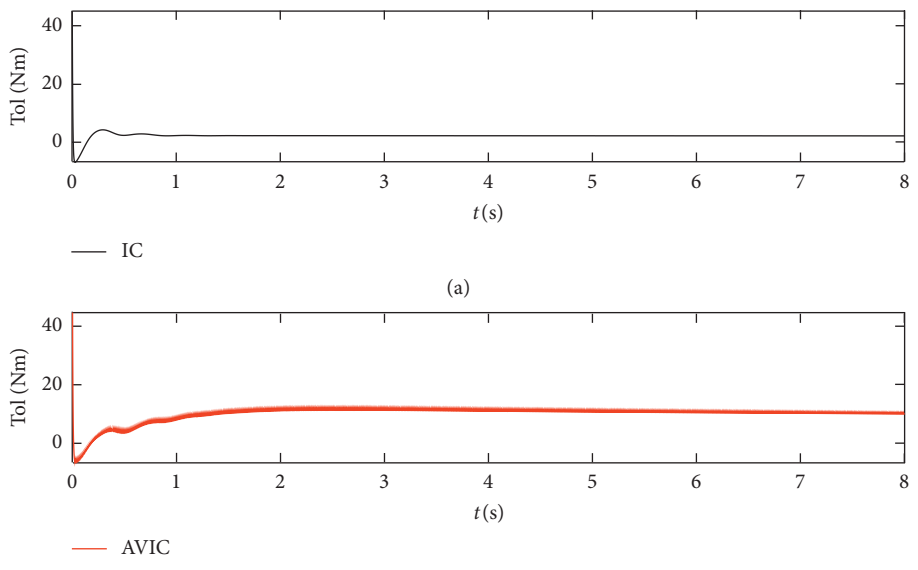

Figure 13: Continued.

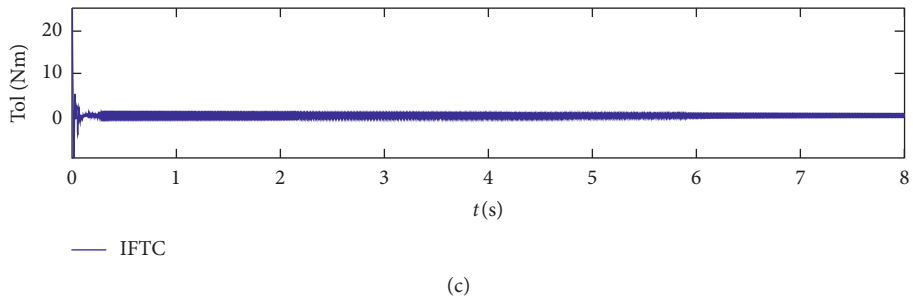

(c)

Figure 13: The torque of the third joint on the slope surface.

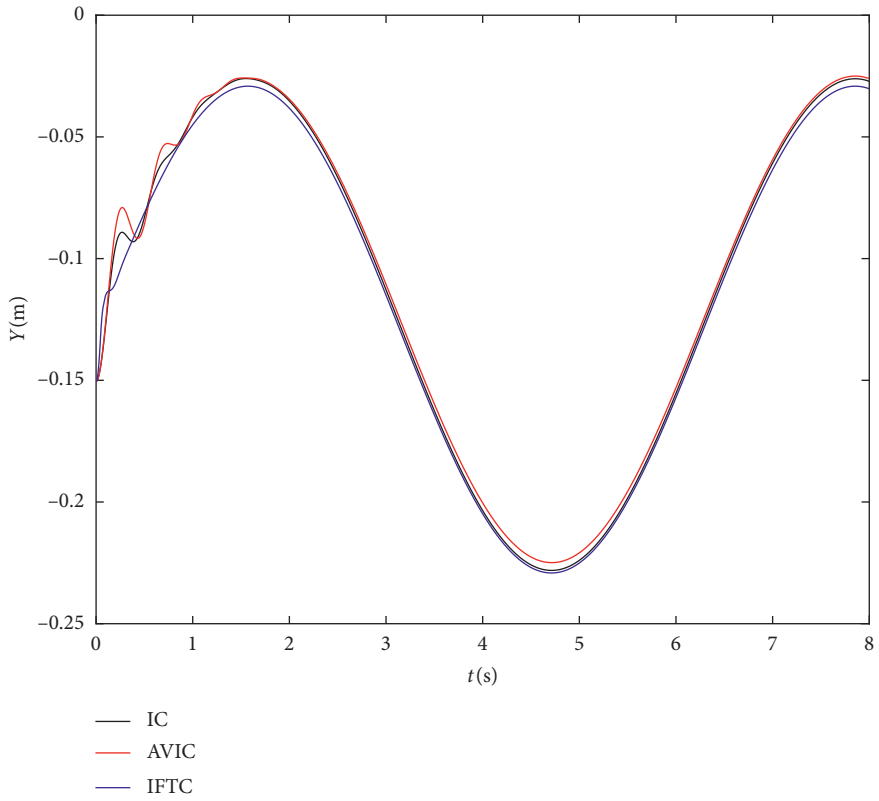

Figure 14: Position tracking of IC on the sinusoidal surface.

4.1. Force/Position Tracking on Planes. When the contact surface between the robot and the environment is plane, the position of the contact surface X_e can be expressed by the following equation: $\ddot{X}_e = 0$, $\dot{X}_e = 0$, $X_e = -0.130$. In this simulation, in order to verify the working state of the robot in different contact surfaces, we assume that the stiffness of the contact surface will change. Therefore, the damping coefficient and stiffness coefficient of the environmental contact surface can be expressed as $B_e = \text{diag}([0, 2, 0, 0, 0, 0]); 0 < t \le 2$, $K_e = \text{diag}([0, 1000, 0, 0, 0, 0]); 2 < t \le 4$, $K_e = \text{diag}([0, 3000, 0, 0, 0, 0]); 4 < t \le 6$, $K_e = \text{diag}([0, 5000, 0, 0, 0, 0]); 4 < t$, and $K_e = \text{diag}([0, 7000, 0, 0, 0, 0])$.

The simulation results are shown in Figures 2–7. Figures 2 and 3, respectively, show the position tracking trajectory and position error of the three control algorithms. It can be seen that they all can get satisfactory results by adjusting the control parameters at 1.2 s, 1.5 s, and 0.6 s, respectively, for the IC, AVIC, and IFTC. Compared with the IC and AVIC, the biggest advantage of the IFTC is that there is no position overshoot, which is a very good phenomenon for the contact between robot end and environment. Figure 4 shows the contact forces of the three control algorithms, in which the IC has no ability to track the contact forces, while the IFTC algorithm has the least force oscillation. Figures 5–7, respectively, represent the control signals of the first three joints, i.e., the joint torque obtained by the control algorithm.

4.2. Force/Position Tracking on the Slope Surface. When the contact surface between the robot and the environment is

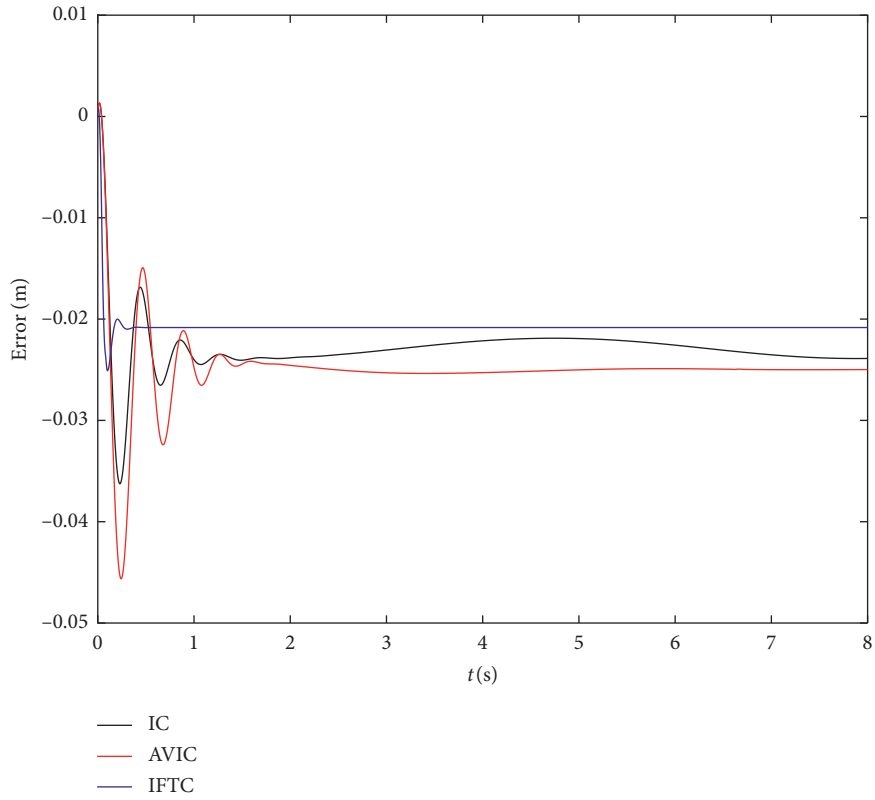

Figure 15: The trajectory tracking error on the sinusoidal surface.

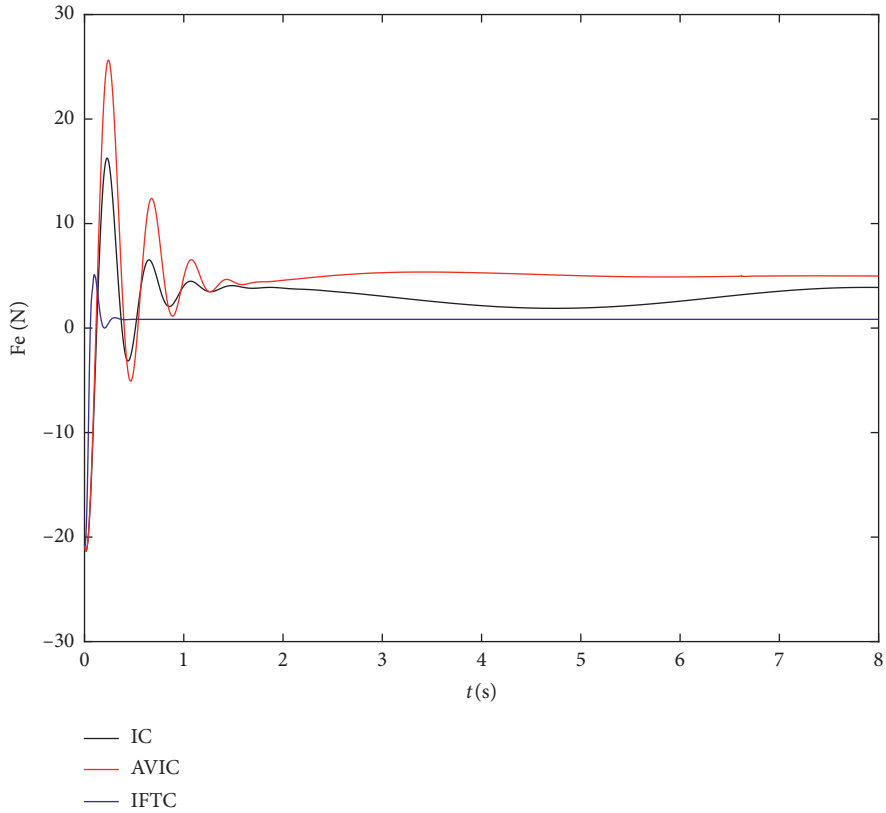

Figure 16: Force tracking on the sinusoidal surface.

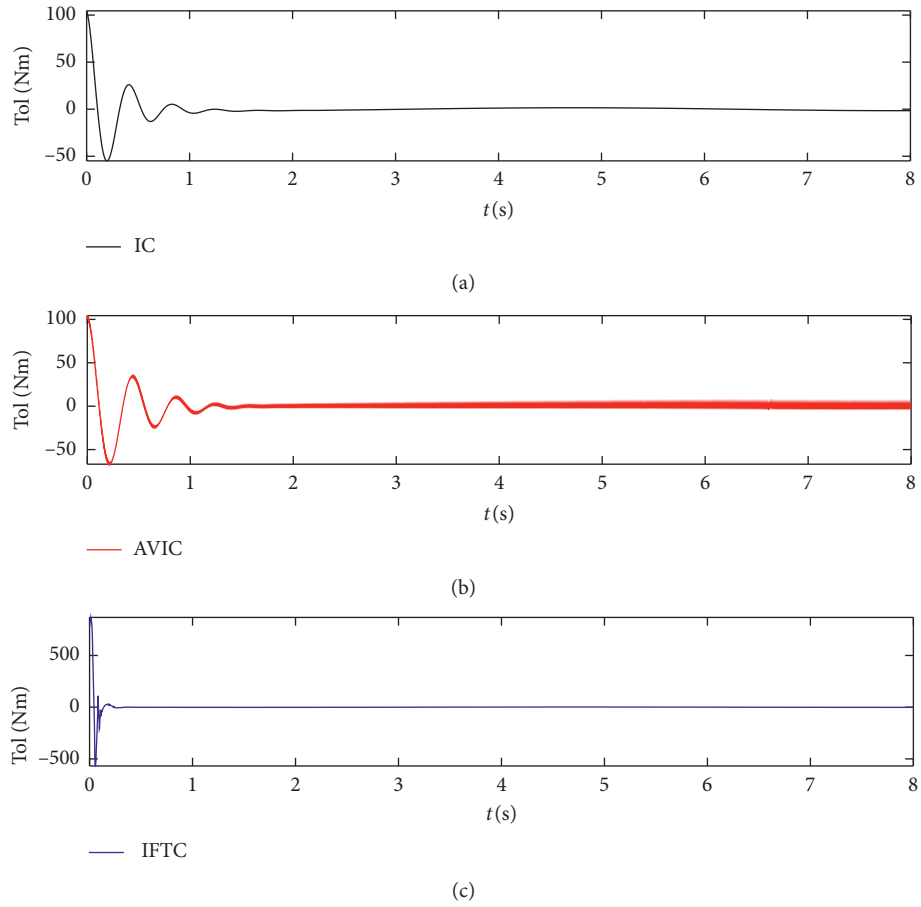

Figure 17: The torque of the first joint on the sinusoidal surface.

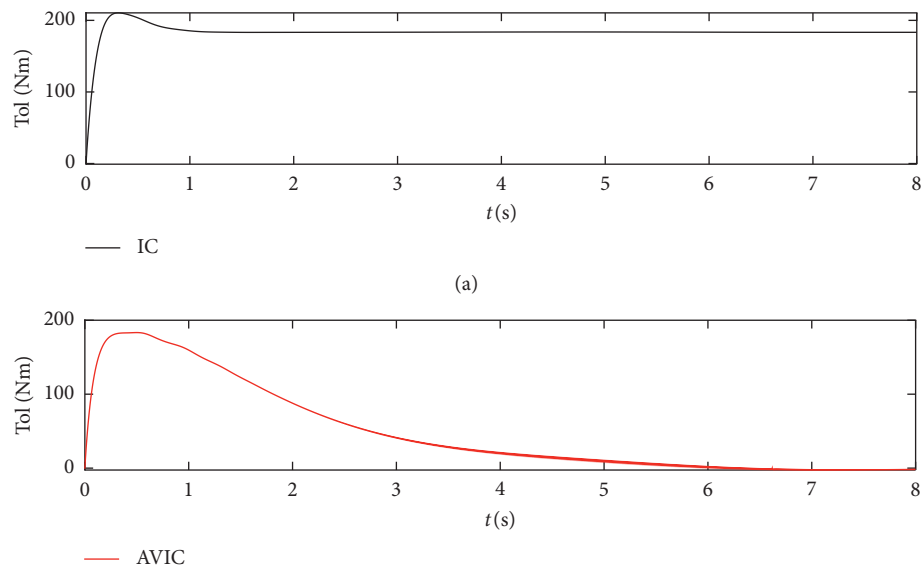

Figure 18: Continued.

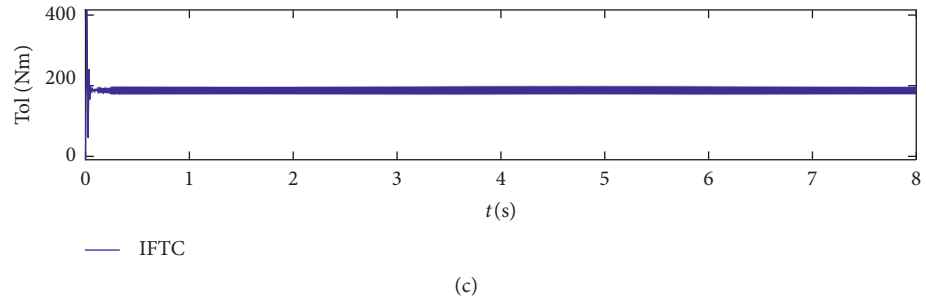

(c)

Figure 18: The torque of the second joint on the sinusoidal surface.

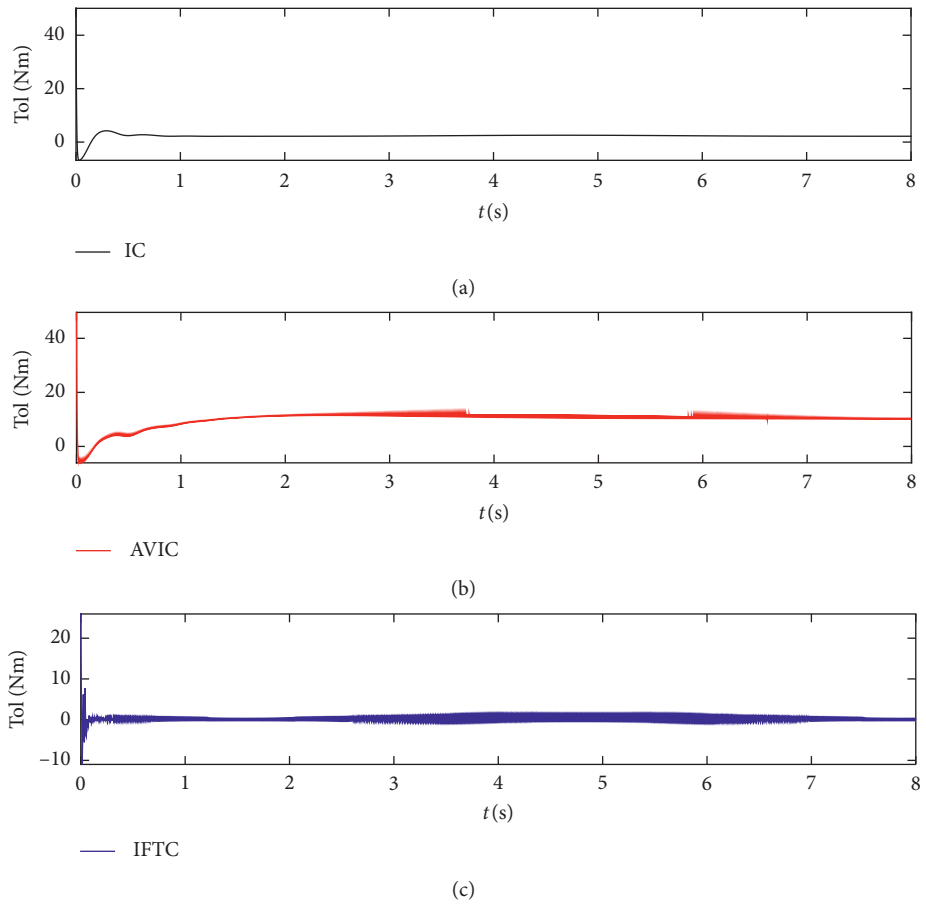

Figure 19: The torque of the third joint on the sinusoidal surface.

slope, we assume that the environment position is $\ddot{X}_e = 0$, $\dot{X}_e = 0.01$, $X_e = -0.130 + 0.01t$. At the beginning of the simulation, the robot has been in full contact with the environment. The damping coefficient and stiffness coefficient of the environment are $B_e = \mathrm{diag}([0, 2, 0, 0, 0, 0])$; $K_e = \mathrm{diag}([0, 1000, 0, 0, 0, 0])$.

The purpose of this simulation is to verify and compare the performance of three control algorithms when the robot moves in a slowly changing environment. Figures 8 and 9 show the position tracking trajectory and position error of the robot. The stable tracking time of the three control algorithms (IC, IFTC, and AVIC) is 1.2 s, 0.3 s, and 1.4 s, respectively. We can conclude that the IFTC algorithm has the shortest stable time and the smallest error. Figure 10 shows the contact force, and it can be seen that the IFTC algorithm first reaches the force stable state. Figures 11–13, respectively, represent the control signals of the first three joints, i.e., the joint torque obtained by the control algorithm.

4.3. Force/Position Tracking on the Sinusoidal Surface. When the contact surface is sinusoidal, the location of the environment X_e is selected: $\ddot{X}_e = -0.01\sin(t)$, $\dot{X}_e = 0.01\cos(t)$, $X_e = -0.130 + 0.01\sin(t)$. In order to

achieve better results, the starting point of the end of the manipulator is in contact with the environment. The coefficient of the environment is as follows: $B_e = \text{diag}([0, 2, 0, 0, 0, 0]); K_e = \text{diag}([0, 1000, 0, 0, 0, 0])$.

The purpose of these simulations is to test the robustness of the three methods for position tracking and force tracking on complex surfaces (sinusoidal surfaces as an example). Figures 14 and 15 show the position tracking results and their errors. All of the three methods can achieve good results at 1.0 s, 1.4 s, and 0.4 s, respectively, for IC, AVIC, and IFTC. Figure 16 shows the force tracking results. The contact force of IFTC is the most stable. Figure 17, Figure 18, and Figure 19 are the joint torque control signals, from which it can be seen that AVIC even appears severe vibration. The simulation results show that IFTC has good robustness.

5. Discussion

The above simulation results show that, under different environment conditions, the three control algorithms can achieve satisfactory position tracking effect; from the above three groups, we can draw the following conclusions. First of all, these three control methods can make the robot track the given trajectory. If the appropriate parameters are set, the satisfactory tracking effect can be obtained. Secondly, for the classical impedance control algorithm, it does not have the ability of force tracking. Thirdly, since AVIC mainly focuses on the tracking of contact force in the design of control strategy, the setting of the impedance parameter should be considered, when using; otherwise, the system will be unstable; from the simulation results, the force tracking results of IFTC are better.

The simulation results show that the control method can achieve good tracking effect in both uncertain environment and uncertain model.

6. Conclusion

Aiming at the position/force control problem of the robot when the model and position are uncertain, this paper proposes a new method of impedance with finite-time control. The introduction of finite-time control ensures the stability of the system in finite time. On the one hand, it improves the response speed; on the other hand, it ensures the tracking accuracy and has better robustness and anti-interference performance. It does not need the complex dynamics knowledge of the robot, and the calculation is simple. Theoretical analysis and simulation results show that the control method proposed by the authors is effective. The effectiveness of the algorithm is proved by a series of simulations. Furthermore, a real robot platform is being built, after which the algorithm will be strictly verified by experiments.

Data Availability

The data used to support the findings of this study are available from the corresponding author upon request.

Conflicts of Interest

The authors declare that they have no conflicts of interest.

References

[1] J. Sanchez, J.-A. Corrales, B.-C. Bouzgarrou, and Y. Mezouar, "Robotic manipulation and sensing of deformable objects in domestic and industrial applications: a survey," *The International Journal of Robotics Research*, vol. 37, no. 7, pp. 688–716, 2018.

[2] B. Vanderborght, A. Albu-Schaeffer, A. E. Bicchi et al., "Variable impedance actuators: a review," *Robotics and Autonomous Systems*, vol. 61, no. 12, pp. 1601–1614, 2013.

[3] N. Hogan, "Impedance control: an approach to manipulation: part I-theory," *Journal of Dynamic Systems, Measurement, and Control*, vol. 107, no. 1, pp. 1–7, 1985.

[4] M. H. Raibert and J. J. Craig, "Hybrid position/force control of robot manipulators," *Journal of Dynamic Systems, Measurement, and Control*, vol. 103, no. 2, pp. 126–133, 1981.

[5] A. Calanca, R. Muradore, and P. Fiorini, "A review of algorithms for compliant control of stiff and fixed-compliance robots," *ASME Transactions on Mechatronics*, vol. 21, no. 2, 2016.

[6] H. Seraji and R. Colbaugh, "Force tracking in impedance control," *The International Journal of Robotics Research*, vol. 16, no. 1, pp. 97–117, 1993.

[7] S. Jung and T. C. Hsia, "Robust neural force control scheme under uncertainties in robot dynamics and unknown environment," *IEEE Transactions on Industrial Electronics*, vol. 47, no. 2, pp. 403–412, 2002.

[8] S. Jung, T. C. Hsia, and R. G. Bonitz, "Force tracking impedance control of robot manipulators under unknown environment," *IEEE Transactions on Control Systems Technology*, vol. 12, no. 3, pp. 474–483, 2004.

[9] S. Jung and T. C. Hsia, "Force tracking impedance control of robot manipulators for environment with damping," in *Proceedings of the IECON 2007—33rd Annual Conference of the IEEE Industrial Electronics Society*, Taipei, Taiwan, November 2007.

[10] J. Duan, Y. Gan, M. Chen, and X. Dai, "Adaptive variable impedance control for dynamic contact force tracking in uncertain environment," *Robotics and Autonomous Systems*, vol. 102, pp. 54–65, 2018.

[11] Y. Dong and B. Ren, "UDE-based variable impedance control of uncertain robot systems," *IEEE Transactions on Systems, Man, and Cybernetics: Systems*, vol. 49, no. 12, pp. 2487–2498, 2019.

[12] Y. Li and S. S. Ge, "Impedance learning for robots interacting with unknown environments," *IEEE Transactions on Control Systems Technology*, vol. 22, no. 4, pp. 1422–1432, 2014.

[13] T. Valency and M. Zacksenhouse, "Accuracy/robustness dilemma in impedance control," *ournal of Dynamic Systems, Measurement, and Control*, vol. 125, no. 3, pp. 310–319, 2003.

[14] J. Baek, M. Jin, and S. Han, "A new adaptive sliding-mode control scheme for application to robot manipulators," *IEEE Transactions on Industrial Electronics*, vol. 63, no. 6, pp. 3628–3637, 2016.

[15] S. Yu, X. Yu, B. Shirinzadeh, and Z. Man, "Continuous finite-time control for robotic manipulators with terminal sliding mode," *Automatica*, vol. 41, no. 11, pp. 1957–1964, 2005.

[16] L. Zhang, L. Liu, Z. Wang, and Y. Xia, "Continuous finite-time control for uncertain robot manipulators with integral sliding

mode," *IET Control Theory & Applications*, vol. 12, no. 11, pp. 1621–1627, 2018.

[17] J. Peng, Z. Yang, and T. Ma, "Position/force tracking impedance control for robotic systems with uncertainties based on adaptive jacobian and neural network," *Complexity*, vol. 2019, Article ID 1406534, 16 pages, 2019.

[18] I. Bonilla, M. Mendoza, D. U. Campos-Delgado, and D. E. Hernández-Alfaro, "Adaptive impedance control of robot manipulators with parametric uncertainty for constrained path-tracking," *International Journal of Applied Mathematics and Computer Science*, vol. 28, no. 2, pp. 363–374, 2018.

[19] G. I. Zamora-Gómez, A. Zavala-Río, D. J. López-Araujo, E. Nuño, and E. Cruz-Zavala, "Further advancements on the output-feedback global continuous control for the finite-time and exponential stabilisation of bounded-input mechanical systems: desired conservative-force compensation and experiments," *International Journal of Control*, pp. 1–13, 2018.

[20] E. Cruz-Zavala, E. Nuño, and J. A. Moreno, "Continuous finite-time regulation of Euler-Lagrange systems via energy shaping," *International Journal of Control*, pp. 1–10, 2019.

[21] J. Lee, P. H. Chang, and M. Jin, "Adaptive integral sliding mode control with time-delay estimation for robot manipulators," *IEEE Transactions on Industrial Electronics*, vol. 64, no. 8, pp. 6796–6804, 2017.

[22] B. Wang, S. Li, and Q. Chen, "Robust adaptive finite-time tracking control of uncertain mechanical systems with input saturation and deadzone," *Transactions of the Institute of Measurement and Control*, vol. 41, no. 2, pp. 560–572, 2019.

[23] G. I. Zamora-Gomez, A. Zavala-Rio, D. J. Lopez-Araujo, E. Cruz-Zavala, and E. Nuño, "Continuous control for fully-damped mechanical systems with input constraints: finite-time and exponential tracking," *IEEE Transactions on Automatic Control*, vol. 65, no. 2, pp. 882–889, 2020.

[24] S. P. Bhat and D. S. Bemstein, "Finite-time stability of homogeneous systems," in *Proceedings of the American Control Conference (Cat. No.97CH36041)*, pp. 2513-2514, Albuquerque, NM, USA, June 1997.

[25] S. P. Bhat and D. S. Bernstein, "Finite-time stability of continuous autonomous systems," *SIAM Journal on Control and Optimization*, vol. 38, no. 3, pp. 751–766, 2000.

[26] Y. Hong, J. Wang, and D. Cheng, "Adaptive finite-time control of nonlinear systems with parametric uncertainty," *IEEE Transactions on Automatic Control*, vol. 51, no. 5, pp. 858–862, 2006.

[27] M. Jin, J. Lee, and P. H. Chang, "Practical nonsingular terminal sliding-mode control of robot manipulators for high-accuracy tracking control," *IEEE Transactions on Industrial Electronics*, vol. 56, no. 9, pp. 3593–3601, 2009.

[28] Y. Hong, Y. Xu, and J. Huang, "Finite-time control for robot manipulators," *Systems & Control Letters*, vol. 46, no. 4, pp. 243–253, 2002.

[29] Y. Su, "Global continuous finite-time tracking of robot manipulators," *International Journal of Robust and Nonlinear Control*, vol. 19, no. 17, pp. 1871–1885, 2009.

[30] Y. Su and C. Zheng, "Global finite-time inverse tracking control of robot manipulators," *Robotics and Computer-Integrated Manufacturing*, vol. 27, no. 3, pp. 550–557, 2011.

[31] N. K. Ruchika and N. Kumar, "Finite time control scheme for robot manipulators using fast terminal sliding mode control and RBFNN," *International Journal of Dynamics and Control*, vol. 7, no. 2, pp. 758–766, 2019.

[32] C. Yang, T. Teng, B. Xu, Z. Li, J. Na, and C.-Y. Su, "Global adaptive tracking control of robot manipulators using neural networks with finite-time learning convergence," *International Journal of Control, Automation and Systems*, vol. 15, no. 4, pp. 1916–1924, 2017.

[33] S. J. Gambhire, K. S. Sri Kanth, G. M. Malvatkar, and P. S. Londhe, "Robust fast finite-time sliding mode control for industrial robot manipulators," *International Journal of Dynamics and Control*, vol. 7, no. 2, pp. 607–618, 2019.

[34] P. Cao, Y. Gan, and X. Dai, "Finite-time disturbance observer for robotic manipulators," *Sensors*, vol. 19, no. 8, p. 1943, 2019.

[35] M. Jin, S. H. Kang, and P. H. Chang, "Robust compliant motion control of robot with nonlinear friction using time-delay estimation," *IEEE Transactions on Industrial Electronics*, vol. 55, no. 1, pp. 258–269, 2008.

[36] S. Ding, S. Li, and Q. Li, "Stability analysis for a second-order continuous finite-time control system subject to a disturbance," *Journal of Control Theory and Applications*, vol. 7, no. 3, pp. 271–276, 2009.